Relative Affinity of Bambus[6]uril Towards Halide Ions: A DFT/GIAO Approach in the Gas Phase, and in the Presence of the Solvent Employing Discrete and Discrete-Continuum Models

ARTICLE *in* COMPUTATIONAL AND THEORETICAL CHEMISTRY · APRIL 2015

Impact Factor: 1.55 · DOI: 10.1016/j.comptc.2015.03.028

2 AUTHORS:

Jorge S. Gancheff
University of the Republic, Uruguay
45 PUBLICATIONS **337** CITATIONS
SEE PROFILE

Pablo A. Denis
University of the Republic, Uruguay
104 PUBLICATIONS **1,559** CITATIONS
SEE PROFILE

Computational and Theoretical Chemistry 1064 (2015) 35–44

Contents lists available at ScienceDirect

Computational and Theoretical Chemistry

journal homepage: www.elsevier.com/locate/comptc

Relative affinity of bambus[6]uril towards halide ions: A DFT/GIAO approach in the gas phase, and in the presence of the solvent employing discrete and discrete-continuum models

Jorge S. Gancheff [a,*], Pablo A. Denis [b]

[a] Cátedra de Química Inorgánica, Departamento "Estrella Campos", Facultad de Química, Universidad de la República, CC 1157, 11800 Montevideo, Uruguay
[b] Computational Nanotechnology, DETEMA, Facultad de Química, Universidad de la República, Montevideo, Uruguay

ARTICLE INFO

Article history:
Received 6 February 2015
Accepted 25 March 2015
Available online 28 April 2015

Keywords:
Supramolecular chemistry
Host–guest complexes
DFT
GIAO

ABSTRACT

The affinity of bambus[6]uril (BU[6]) towards halides ($X^- = F^-$, Cl^-, Br^-, I^-) is investigated employing the DFT/GIAO approach with B3LYP and M06-2X, and double- (LANL2DZ, MIDI!) and triple-ξ (6-311++G(d,p)) basis sets. Calculations with B3LYP/LANL2DZ are conducted in the gas phase and in the presence of methanol as solvent employing discrete (two and six molecules) and continuum-discrete models. B3LYP has proven to outperform the behavior of M06-2X. The observed affinity in going from chloride to iodide is correctly described with B3LYP/LANL2DZ in the gas phase: these anions are hosted preferentially in the order $I^- > Br^- > Cl^-$. However, fluoride emerged as the preferred guest in contraposition to the experimental findings. The inclusion of the solvent or the use of large basis, rather to improve the result of affinity in the gas phase, worsens it. Finally, B3LYP/LANL2DZ/GIAO in the gas phase is recommended as a tool to assist experimentalists in studying relative affinities in encapsulation processes of similar guests keeping the computational cost very low.

1. Introduction

Non-covalent interactions are ubiquitous in chemistry. The insights derived from fundamental study of non-covalent interactions have been successfully employed in a wide range of applications including self-assembly of nanostructures, development of catalysts, and selective encapsulation of different ions and molecules in solution [1–6]. The ability of receptors to interact with guests with high affinity as a result of highly selective binding processes is a requirement for all these applications. In response, supramolecular chemists have directed their efforts to synthesize an important variety of non-natural receptors displaying exceptional affinities and selectivities. A representative example of such receptors is a family of supramolecular hosts called cucurbit[*n*]urils (CB[n]), named for its peculiar pumpkin-like structure. These molecules are afforded by the condensation of glycoluril and formaldehyde in strongly acidic solutions [3,7]. Even when the first cucurbituril (CB[6]) was synthesized in 1905 by Behrend and co-workers [8], its structure was not determined until 1981 [9]. Other members of the CB[n] family were simultaneously yielded during the preparation of CB[6], but they were not identified or studied until 2000 [10]. Since their discovery, the development of new CB-derivatives received major attention and still represents an open field of research. Indeed, the synthesis of a six-membered macrocycle (bambus[6]uril, BU[6]) has recently reported by Svec and co-workers [5]. This macrocyle has six glycouril units connected through methylene bridges and can be viewed as a structure derived from cucurbit[6]uril and hemicucurbit[6]uril. BU[6] showed a good affinity towards halide ions. Such anions are hosted preferentially in the order $I^- > Br^- > Cl^-$ > and F^-, as observed by ^{1}H NMR investigations [5,11]. The crystallographic structures of complexes Cl^-@BU[6] and Br^-@BU[6] revealed halides hosted as product of weak hydrogen bonds between the twelve methinic units on the convex face of glycoluril units and the corresponding anion [5]. Theoretical calculations have been recently employed to go deep into insight the understanding of these interactions [12–16]. In particular, we showed that the gas phase affinity of BU[6] for halides differs from that observed in solution, as the strongest interaction was observed for fluoride [12,13]. However, this trend is in line with the calculated hydrogen bond energies between halides and alkane, olefiens, and parafines [13]. The difficulty in the prediction of the interaction energies, and the high selectivity of BU[6] for halides motivated us to conduct a ^{1}H NMR theoretical investigation of the relative affinity experimentally observed. We note that the

* Corresponding author. Tel.: +598 2924 9739; fax: +598 2924 1906.
E-mail address: jorge@fq.edu.uy (J.S. Gancheff).

http://dx.doi.org/10.1016/j.comptc.2015.03.028
2210-271X/

recent work by Gobre et al. [15] studied the ^{1}H NMR shifts for complexes with fluoride, chloride, and bromide. However, the most relevant one – iodide – was not considered. Thus, we consider that it is important to extend the work and include iodide, which is the preferred guest.

Our efforts are focused on the shift of the resonance signal of the H-atoms directly involved in the interaction host–guest. Herein, is our aims twofold: (a) to test the behavior of standard DFT methods in studying relative affinities in know host–guest complexes, and (b) to shed light into the interaction between halide ions and BU[6]. In doing so, we expect to find a theoretical tool with low computational cost able to assist experimentalist in studying relative affinities in encapsulation complexes.

2. Computational details

All calculations were undertaken at the density functional theory (DFT) level of theory. It has been reported that hybrid functionals have proven to be better performers in accurately predict ^{1}H chemical shift than pure functionals [17]. Therefore, we focused our attention on the popular B3LYP functional [18–20]. The functional M06-2X [21] – featured by a well performance in dealing with non-covalent interactions [22–24] – was also included in this study with the aim to explore its feasibility in predicting ^{1}H NMR shifts in host–guest complexes. It is worth mentioning that the ability of M06-2X in studying thermodynamic aspects of encapsulation processes of BU[6] toward halide ions has been recently evaluated by us [12,13].

The combination of a hybrid functional with a basis set of at least 6-31G(d) quality has been proposed as sufficient to reasonably reproduce ^{1}H chemical shifts [25,26]. However, the inclusion of bromide and iodide in this contribution does not allow us to employ 6-31G(d). This observation prompted us to use double-ξ basis set large enough to ensure a low computational cost for all systems covered in this study. In this regard, LANL2DZ and MIDI! were taken into account. To explore the effect of the basis, 6-311G was also considered. With the inclusion of this triple-ξ basis set, an affordable computational cost for all complexes/conformers studied has been obtained. It is important to emphasize that our intention herein is to obtain a theoretical tool of low-cost able to predict *relative affinities* in encapsulation processes.

In order to calculate the chemical shifts, we have followed this procedure:

(1) The geometry of BU[6], and of complexes X^-@BU[6] (X^- = Cl^-, Br^- and I^-) were optimized in the D_{3d}, S_6, and C_1 symmetry point groups (see Fig. 1; further details in Supplementary Material). The encapsulation of fluoride promotes an important distortion of the host as previously observed by us in studying thermodynamic aspect of hosting halides by BU[6] [12,13]. Therefore, only the symmetry C_1 was considered for F^-@BU[6].
(2) The nature of the stationary point was verified through an analytical vibrational analysis (no imaginary frequencies at the minimum).
(3) Isotropic-shielding tensor values for H-atoms ($\sigma_{H,BU[6]}$ for bambus as example) were calculated in the framework of the GIAO methodology [25,27–30].
(4) At the same level of theory as the one considered for the molecule under study, the geometry of tetramethylsilane (TMS, taken as reference as in the experiments) [5] was

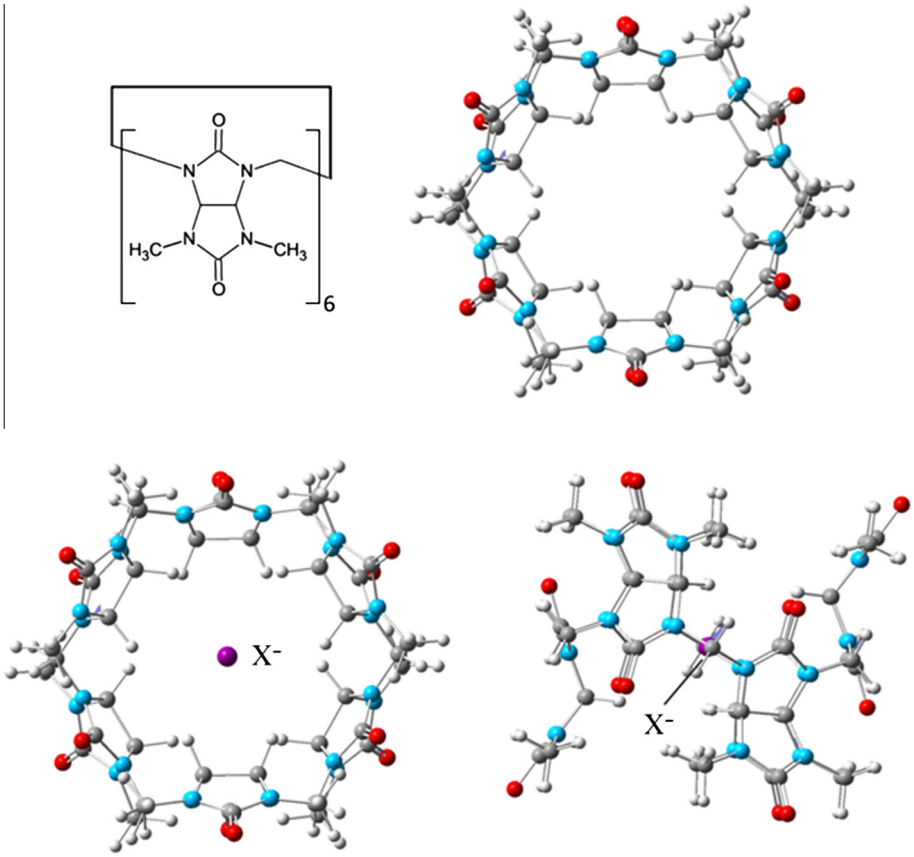

Fig. 1. Geometry of BU[6] (top), and of the encapsulation complexes X^-@BU[6] (X^- = Cl^-, Br^-, I^-) (bottom) studied in the D_{3d}, S_6, and C_1 symmetry point groups employing B3LYP and M06-2X in combination with different basis sets.

optimized, and the nature of the stationary point verified as abovementioned in (2). Isotropic-shielding tensor values for H-atoms ($\sigma_{H,TMS}$) were calculated as in (3).

(5) Once the results of steps (3) and (5) are obtained, the chemical shift is calculated as the difference between them, i.e.:

$$\delta_{H,BU[6]}(\text{ppm}) = \sigma_{H,TMS} - \sigma_{H,BU[6]}$$

In first instance, all geometry optimizations were performed employing the standard integration grid (75,302), for which many transition states (TS) were obtained (further details in Section 3). Hence, we employed also an ultrafine grid featured by 99 radial shells and 590 angular points per shell, which helped us in some cases to reach minima instead TS.

Geometry optimization and GIAO ^{1}H NMR calculations of complexes X^-@BU[6] (X^- = F^-, Cl^-, Br^-, I^-) in the presence of the solvent were also performed. Our aim herein is to explore the influence of non-covalent interaction between guest and the solvent on ^{1}H NMR signals, in particular, on the ones associated to methinic protons. By doing so, we expect to obtain a clear picture of the influence of the solvent on the *relative affinity* of BU[6] towards halides. Besides, this approach will help us to evaluate the reliability of our results in the gas phase. ^{1}H NMR measurements have been conducted in CH_3OH-d_4:$CHCl_3$-d (2:1, v:v) [5]. Therefore, we decided to take methanol as solvent into account.

The presence of the solvent was taken through two models into account:

1. A discrete model including two and six methanol molecules to the geometry of BU[6]. In both cases, two solvent molecules (denoted as "s" in figures) have been initially placed at both portal of the macrocycle interacting with the hosted ion. Additional four solvent units aiming at solvating the portals are also included.
2. A discrete-continuum model (including two and six methanol molecules to the geometry of BU[6] interacting with halide ions) in which the continuum was modeled with the C-CPM [31,32] approach.

All theoretical results reported herein were obtained using the program package GAUSSIAN 09, Rev. D.01 [33].

3. Results and discussion

3.1. Bambus[6]uril, BU[6]

Three conformations featured by the symmetry point groups D_{3d}, S_6, and C_1 have been investigated. The influence of the integration grid on the nature of the stationary point has been studied by employing B3LYP. The combination of this functional with LANL2DZ was in conditions to found a minimum as stationary point for all conformations (Table 1), regardless the integration grid. B3LYP in conjunction with the other double-ξ basis sets considered (MIDI! and 6-31G(d)) was in conditions to reach a minimum instead a TS with the ultrafine grid for the C_1 conformer. When the size of the basis set is increased, all geometry optimizations conducted to a minimum only by using the ultrafine grid.

The largest difference in stability has been obtained with B3LYP/LANL2DZ (fine grid), for which the C_1 conformer appears as more stable by 4.24 kcal/mol with respect to the S_6 one (Supplementary Material Table S1).

To conduct optimizations of the host, the ultrafine grid seems to be a better choice than the standard one. Thus, we decided to perform all NMR investigation for the host and all halide-containing complexes by employing an ultrafine integration grid. The chemical shifts have been calculated for the H-atoms responsible of the weak H-bond observed when the halides are hosted, namely, the methinic hydrogens at the convex face of the glycouril units (hereafter referred to as H_c, as in the experiments) [5].

Table 1
Optimization results of BU[6] as obtained using B3LYP and different basis sets (T = 298 K).[a,b]

Basis set	Symmetry point group	Fine grid	Ultrafine grid
LANL2DZ	D_{3d}	M	M
	S_6	M	M
	C_1	M	M
MIDI!	D_{3d}	TS	TS
	S_6	M	M
	C_1	TS	M
6-31(d)	D_{3d}	TS	TS
	S_6	M	M
	C_1	TS	M
6-311G	D_{3d}	TS	M
	S_6	M	M
	C_1	M	M

[a] M = minimum; TS = transition state.
[b] Fine grid: (75,302) integration grid; ultrafine grid: (99,590) integration grid.

Table 2
Chemical shift (in ppm) of the methinic H-atoms of BU[6] (TMS as reference) as obtained using B3LYP in combination with different basis sets and an ultrafine grid (T = 298 K)[a].

Basis set	Symmetry point group	δ_{Hc}
LANL2DZ	D_{3d}	4.93
	S_6	4.94
	C_1	4.94
MIDI!	D_{3d}	
	S_6	4.20
	C_1	4.22
6-31G(d)	D_{3d}	
	S_6	5.09
	C_1	5.09
6-311G	D_{3d}	4.99
	S_6	5.02
	C_1	5.07

[a] TS has been located for conformers with no value of δ_{Hc}.

The values of δ_{Hc} (ppm) obtained by employing the ultrafine integration grid, and all basis sets considered in this work combined with B3LYP are gathered in Table 2.

Despite our aim to conduct studies of relative affinities, is it worth discussing in few words the performance of each methodology in reproducing the experimental NMR results of BU[6] (δ_{Hc} = 5.51 ppm) [5]. B3LYP in combination with double-ξ basis set leads to values of δ_{Hc} in the range 4.20–5.09 ppm. While LANL2DZ shows reasonable shifts for all conformers, MIDI! clearly represents the worst option. 6-31G(d) seems to be a reasonable performer with a value 0.42 ppm high-field shifted with respect to the experimental evidence. This result has been not remarkable improved by the introduction of the triple-ξ basis set considered. The chemical shift of H_c obtained with 6-31G(d) and 6-311G are in reasonable concordance with the theoretical value reported by Gobre and co-workers of 5.2 ppm at the B3LYP/6-31+G(d,p) level in the presence of DMSO as solvent [15].

The inclusion of diffuse functions by using B3LYP/6-31+G(d) on the D_{3d} conformer resulted in a value for δ_{Hc} of 5.55 ppm, almost identical to the experimental one [5]. The improvement seen when diffuse functions are added is in line with the one made available by Jain and co-workers [17], which focused their efforts to

Table 3
Chemical shift (in ppm) of the methinic H-atoms of BU[6] (TMS as reference) as obtained using M06-2X in combination with different basis sets and an ultrafine grid (T = 298 K).[a]

Basis set	Symmetry point group	δ_{Hc}
LANL2DZ	D_{3d}	4.74
	S_6	4.74
	C_1	4.71
MIDI!	D_{3d}	
	S_6	4.28
	C_1	4.43
6-31G(d)	D_{3d}	
	S_6	
	C_1	4.64
6-311G	D_{3d}	4.93
	S_6	4.93
	C_1	4.93

[a] TS has been located for conformers with no value of δ_{Hc}.

calculate accurate proton chemical shift of several organic molecules with a large set of DFT methods. Table 3 sums up the results obtained with M06-2X.

A close inspection of the results exhibited in Table 3 reveals a poor ability of M06-2X in reproducing ^{1}H NMR results for BU[6]. This functional outperformed B3LYP only combined with MIDI! However, these results are featured by important deviations with respect to the experimental value [5].

The behavior of M06-2X in reproducing proton chemical shift observed by us in this contribution is in line, for instance, with the one reported by Espinoza-Hicks and co-workers in regard to theoretical studies of a novel synthetic prenylated chalcone [34].

The effects of the solvent on geometry and ^{1}H NMR signals of the methinic protons of BU[6] were investigates by means of two approaches: a discrete model with explicit methanol molecules, and a discrete-continuum(C-PCM) [31,32] model. The geometry of BU[6](MeOH)$_2$ and BU[6](MeOH)$_6$ were optimized with B3LYP/LANL2DZ in the gas phase, and in the presence of a continuum with ε of 32.613 (methanol as solvent). Fig. 2 displays the optimized geometry of BU[6](MeOH)$_2$, which also contains the one calculated for the C_1 conformer with B3LYP/LANL2DZ for comparison purposes.

The explicit presence of the solvent does no promote important modifications on the structure of the macrocycle. The optimized geometry of BU[6](MeOH)$_2$ shows methanol at the portal of BU[6] interacting *via* H-bond with an oxygen of a glycouril unit with a distance HO–H···O of 1.723 Å. This finding supports the proposed hydrophobic nature of the cavity, as stated by Dixit and co-workers [35]. The structure of complex BU[6](MeOH)$_2$ minimized in the presence of the continuum does not show any important deviation with respect to the one in the gas phase.

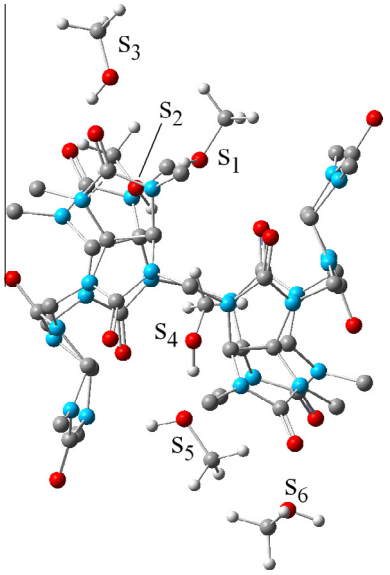

Fig. 3. Optimized geometry of BU[6](MeOH)$_6$ as obtained with B3LYP/LANL2DZ. Hydrogen atoms of BU[6] have been omitted for clarity.

When six methanol molecules are explicited, interesting features emerged. The structure of BU[6](MeOH)$_6$ at the minimum is displayed in Fig. 3.

We started considering three methanol molecules interacting with the macrocycle at both portals. At the minimum, three of them (s_1, s_2, s_3) do not noticeably deviated with respect to the initial structure, while – surprisingly – one molecule (s_4) is observed hosted in the BU[6]s cavity interacting through H-bond with s_5 (distance (s_4) H_3CO–H···$OHCH_3$ (s_5) of 1.634 Å). Both s_5 and s_6 remain solvating the environment of the other portal.

The explicit presence of the solvent modifies the ^{1}H NMR signals calculated in the gas phase. Table 4 exhibits the chemical shift of the methinic protons of complexes BU[6](MeOH)$_n$ (n = 2, 6) in the gas phase and in the presence of the continuum.

The standard methodology B3LYP/LANL2DZ delivers a value of δ_{Hc} of 5.52 ppm for BU[6] in the presence of two methanol molecules, which represents an excellent approximation to the experimental value of 5.51 ppm obtained in DMSO-d_6–$CHCl_3$-d (1:1, v:v) [5]. The inclusion of more solvent molecules, rather than to contribute to an improvement of the agreement between calculated and experimental shift, worsens it ($\delta_{Hc,calc.}$ of 5.24 ppm). This finding represents another argument in line with the hydrophobic nature of BU[6]s cavity. The inclusion of the continuum only improves the results for BU[6] and BU[6](MeOH)$_6$ in the gas phase. Even when the shift for BU[6](MeOH)$_2$/CPCM does not resulted so good as the one for BU[6](MeOH)$_2$, it is also

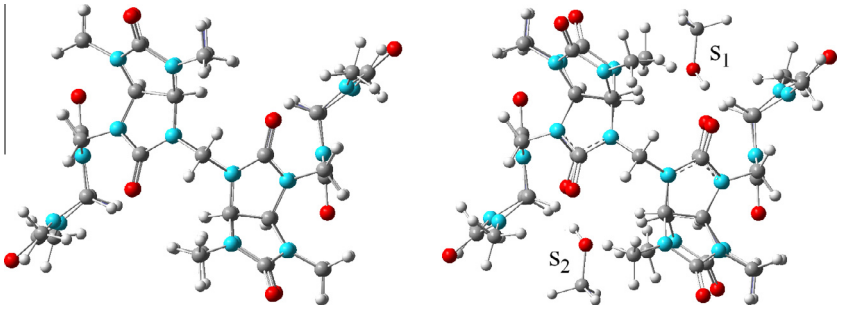

Fig. 2. Optimized geometry of BU[6] (C_1 conformer) (left), and of BU[6](MeOH)$_2$ (right) as obtained with B3LYP/LANL2DZ.

Table 4
Chemical shift (in ppm) of the methinic protons of complexes BU[6](MeOH)$_n$ (n = 2, 6; TMS as reference) as obtained using B3LYP/LANL2DZ and an ultrafine grid (T = 298 K).

Complex	δ_{Hc}	$\Delta\delta_{Hc}$[a]
BU[6]	4.94[b]	0
BU[6](MeOH)$_2$	5.52	0.58
BU[6](MeOH)$_6$	5.30	0.30
BU[6]/CPCM	5.03	0.09
BU[6](MeOH)$_2$/CPCM	5.54	0.60
BU[6](MeOH)$_6$/CPCM	5.48	0.54

[a] $\Delta\delta_{Hc^-} = \delta_{Hc}$ (complex with solvent) – δ_{Hc} (complex without solvent).
[b] Value taken from Table 3, C_1 conformer.

Table 5
Chemical shift (in ppm) for the methinic protons of Cl$^-$@BU[6] as calculated with different functionals and basis sets (T = 298 K).[a]

Functional	Basis set	Conformer	δ_{Hc}	$\Delta\delta_{Cl^-}$[b]
B3LYP	LANL2DZ	D_{3d}	5.13	0.20
		S_6	5.14	0.20
		C_1	5.17	0.23
	MIDI!	D_{3d}		
		S_6	4.88	0.68
		C_1	4.99	0.77
	6-311G	D_{3d}	5.10	0.11
		S_6	5.10	0.08
		C_1	5.13	0.06
M06-2X	LANL2DZ	D_{3d}	5.02	0.28
		S_6	5.07	0.33
		C_1	5.12	0.41
	MIDI!	D_{3d}		
		S_6	5.20	0.92
		C_1	5.15	0.72
	6-311G	D_{3d}	5.06	0.13
		S_6	5.06	0.13
		C_1	5.09	0.16

[a] TS has been located for conformers with no value of δ_{Hc}.
[b] $\Delta\delta_{Cl^-} = \delta_{Hc}$ (Cl$^-$@BU[6]) – δ_{Hc} (BU[6]).

represents a very good approximation to the experimental value with a deviation of +0.03 ppm.

3.2. Inclusion complexes X$^-$@BU[6] (X$^-$ = Cl$^-$, Br$^-$, I$^-$), and relative affinity of BU[6] for Cl$^-$, Br$^-$, and I$^-$ (in the gas phase)

Firstly, the encapsulation of chloride influences the δ_H signals of all protons of BU[6], and of the methinic ones in particular. The results of the change calculated for δ_{Hc} when the halide ion is encapsulated (with respect to the host) employing B3LYP, and M06-2X in combination with LANL2DZ, MIDI! and 6-311G are gathered in Table 5.

When BU[6] interacts with chloride, all DFT methods account for a downfield-shift of the resonance signal of the methinic protons. As can be seen in Table 5, the functional and the basis set affect the magnitude of the shift with values ranging from 0.06 ppm to 0.92 ppm. The conformation of the complex seems to be a variable of least importance.

No experimental value of $\Delta\delta_{Cl^-}$ for Cl$^-$@BU[6] is available. However, the reported shift when bromide is encapsulated and replaces chloride (referred as to $\Delta\Delta\delta_{Br^-}$, see further in text) is of 0.05 ppm [5], BU[6] experimentally showing a lower affinity for chloride with respect to bromide [5]. These observations helped us to assume that LANL2DZ combined with both functionals clearly overestimates the magnitude of the interaction. The overestimation is more pronounced by employing MIDI!, which gives a shift of about 1 ppm (combined with M06-2X, S6 conformer).

The behavior of all DFT methods to study the change in the resonance of the methinic protons when BU[6] interacts with bromide and iodide resulted analogous to the one already commented for Cl$^-$@BU[6] (see Tables S2 and S3 in the Supplementary Material).

Table 6
Relative affinity of halide ions towards BU[6] as evaluated by different GIAO/DFT methods and an ultrafine integration grid (T = 298 K).[a]

Method[b]	Conformer	$\Delta\Delta\delta_{X^-}$ (ppm)[c]		
		I$^-$	Br$^-$	Cl$^-$
BLDZ	D_{3d}	0.15	0.07	0
	S_6	0.14	0.06	0
	C_1	0.11	0.03	0
BMIDI	D_{3d}			
	S_6	0.10	0	0
	C_1	−0.17	−0.22	0
B6311	D_{3d}	0.17	0.06	0
	S_6	0.16	0.06	0
	C_1	0.15	0.05	0
MLDZ	D_{3d}	0.25	0.10	0
	S_6	0.20	0.06	0
	C_1	0.14	0.01	0
MMIDI	D_{3d}			
	S_6	0	0	0
	C_1	0.03	−0.01	0
M6311	D_{3d}	0.22	0.06	0
	S_6	0.16	0.10	0
	C_1	0.18	0.03	0
Exp.[d]		0.19	0.05	0

[a] TS has been located for conformers with no value of δ_{Hc}.
[b] B/M/LDZ = B3LYP/M06-2X/LANL2DZ; B/M/MIDI = B3LYP/M06-2X/MIDI!; B/M/6311 = B3LYP/M06-2X/6-311G.
[c] $\Delta\Delta\delta_{X^-} = (\Delta\delta_{X^-} - \Delta\delta_{Cl^-})$ (in ppm) with X$^-$ = Cl$^-$, Br$^-$, and I$^-$.
[d] Values observed in CH_3OH-d_4:$CHCl_3$-d (2:1; v:v) (taken from Ref. [5]).

We decided to study the relative affinity of BU[6] towards Cl$^-$, Br$^-$, and I$^-$ by calculating the ^{1}H NMR shift of the methinic protons of BU[6] in the presence of these anions. As in the experiments, the magnitude of the downfield shift of the methinic protons reflects the magnitude of the interaction between halides and BU[6] [5]. Table 6 exhibits the DFT/GIAO values of the shift, taking the results of Cl$^-$@BU[6] as reference.

The relative affinity experimentally observed was properly described by B3LYP in combination with LANL2DZ and 6-311G: this receptor binds such anions preferentially in the following order: I$^-$ > Br$^-$ > Cl$^-$ [5]. The induced shift observed when bromide replaces chloride (Br$^-$ → Cl$^-$, $\Delta\Delta\delta_{Br^-}$) is 0.05 ppm (Supporting Information of Ref. [5]). The replacement of chloride by iodide (I$^-$ → Cl$^-$, $\Delta\Delta\delta_{I^-}$) is responsible for the experimental shift of 0.19 ppm.

The standard DFT method B3LYP/LANL2DZ has shown a very good performance (with a low computational cost) in the case of the C_1 conformer in particular: the experimental relative affinity has been corrected reproduced, and at the same time, this DFT method accounts for the magnitude of the affinity: $\Delta\Delta\delta_{I^-}/\Delta\Delta\delta_{Br^-}$ of 3.7 vs. 3.8 (exp.). Furthermore, the values of $\Delta\Delta\delta_{Br^-}$ and of $\Delta\Delta\delta_{I^-}$ (0.03 and 0.11 ppm, respectively) are also in agreement with the experimental evidence. When B3LYP is combined with 6-311G, no significant improvements have been obtained. The results for $\Delta\Delta\delta_{X^-}$ seems to be less affected by the conformer's symmetry with an increase in the size of the basis set employed.

M06-2X, a functional usually employed in studying non-covalent interactions [22–24], delivers results also in line with the experimental findings when combined with LANL2DZ and 6-311G. It is worth mentioning that the magnitude of the interaction was also reproduced with 6-311G (D_{3d} conformation): $\Delta\Delta\delta_{I^-}/\Delta\Delta\delta_{Br^-}$ of 3.7 vs. 3.8 (exp.). The respective values of $\Delta\Delta\delta_{Br^-}$ and of $\Delta\Delta\delta_{I^-}$ (0.06 and 0.22 ppm) resulted also in very good agreement with the experimental evidence [5].

Finally, MIDI! does not lead to results in concordance with the experimental observations when used with all DFT functionals considered in this work. This basis set does not show a systematic behavior. For instance, in conjunction with B3LYP, MIDI! does not account for different affinity of BU[6] towards chloride and bromide in a S_6 conformation. For the lowest-symmetry conformer, negative shifts have been calculated.

3.3. Inclusion complexes X^-@BU[6](MeOH)$_n$ (X^- = Cl^-, Br^-, I^-; n = 2, 6), and relative affinity of BU[6] for Cl^-, Br^-, and I^- (in the presence of the solvent)

The optimized geometries of complexes Cl^-@BU[6](MeOH)$_2$, and Cl^-@BU[6](MeOH)$_6$ (taken as example) are displayed in Fig. 4. The presence of methanol interacting with chloride promotes an expansion and modifications of the symmetry of the cavity, modifications derived from the reported flexibility of the macrocycle [5]. Distances $H_{methinic}\cdots Cl^-$ ranging from 2.87 Å to 3.29 Å were calculated for complex Cl^-@BU[6] with B3LYP/LANL2DZ, while the presence of two solvent molecules leads to values in the range 3.03–3.83 Å. The inclusion of six methanol molecules promotes a more pronounced deformation of the receptor, which leads to distances $H_{methinic}\cdots Cl^-$ in the range 2.75–4.68 Å. Analogous results were obtained for Br^-@BU[6](MeOH)$_n$ and I^-@BU[6](MeOH)$_n$ (n = 2, 6).

The optimized geometry of all complexes displays two methanol at the portals of BU[6] interacting *via* H-bond with the halide ion (X^-). Distances O–H$\cdots X^-$ of 2.133, 2.345, and 2.605 Å were calculated for Cl^-@BU[6](MeOH)$_2$, Br^-@BU[6](MeOH)$_2$, and I^-@BU[6](MeOH)$_2$, respectively.

In complexes with six solvent molecules, the situation resembles de same as the one already discussed: two methanol units remain at the portal of the receptor interacting with the halide *via* H-bond with distances O–H$\cdots X^-$ of 2.123 and 2.214 (Cl^-), 2.357 and 2.434 (Br^-), and 2.606 and 2.713 Å (I^-). The optimization of complexes X^-@BU[6](MeOH)$_n$ (X^- = Cl^-, Br^-, I^-; n = 2, 6) in the presence of a continuum (ε = 32.613) by using the C-PCM [31,32] approach does not lead to relevant structural changes with respect to the one already discussed.

The presence of the solvent also affects the ^{1}H NMR results. In discrete complexes with two and six solvent molecules, the direct interaction methanol–halide-ion promotes a downfield-shift of the resonance signal of the methinic protons in all cases with respect to the "free-of-solvent" complexes (see Table 7).

For Cl^-@BU[6](MeOH)$_2$, the value of δ_{Hc} (5.37 ppm) resulted an excellent simulation of the experimental value (5.36 ppm) observed in CH_3OH-d_4:$CHCl_3$-d (2:1, v:v) [5]. In the case of Br^-@BU[6](H$_2$O)$_2$ and I^-@BU[6](H$_2$O)$_2$, B3LYP/LANL2DZ has also shown an improvement of the results in comparison to the ones of the complexes without solvent.

Whilst a deviation of −0.08 ppm has been calculated for Br^-@BU[6](H$_2$O)$_2$, it has resulted of −0.12 ppm for I^-@BU[6](H$_2$O)$_2$. The inclusion of six water molecules, rather than to contribute to an improvement of the agreement between calculated and experimental shifts, worsens it. In all cases, a clear overestimation of δ_{Hc} has been obtained with values (in ppm) of 5.76 (Cl^-), 5.55 (Br^-), and 5.66 (I^-). The differences in δ_{Hc} between complex-with-solvent and complex-without-solvent calculated with B3LYP/LANL2DZ ($\Delta\delta_{Hc}$, Table 7) suggest that the explicit presence of the solvent plays an important role in reproducing ^{1}H NMR results with low-cost DFT methodologies.

Improvements of the values of δ_{Hc} obtained for discrete solvent models were not observed with the inclusion of the continuum (see Table 8). In complexes with two and six solvent molecules, the inclusion of the continuum promotes a high-field shift of the

Table 7
Chemical shift (in ppm) of the methinic protons of X^-@BU[6](MeOH)$_n$ (X^- = Cl^-, Br^-, I^-; n = 2, 6; TMS as reference) in the gas phase as obtained using B3LYP/LANL2DZ (T = 298 K).

Complex	δ_{Hc}	$\Delta\delta_{Hc}$[a]
Cl^-@BU[6]	5.17[b]	0
Cl^-@BU[6](MeOH)$_2$	5.37	0.20
Cl^-@BU[6](MeOH)$_6$	5.76	0.59
Br^-@BU[6]	5.20[c]	0
Br^-@BU[6](MeOH)$_2$	5.34	0.14
Br^-@BU[6](MeOH)$_6$	5.55	0.35
I^-@BU[6]	5.28[c]	0
I^-@BU[6](MeOH)$_2$	5.43	0.15
I^-@BU[6](MeOH)$_6$	5.66	0.38

[a] $\Delta\delta_{Hc} = \delta_{Hc}$ (complex with solvent) − δ_{Hc} (complex without solvent).
[b] Value taken from Table 5, C_1 conformer.
[c] Values given in Tables S2 and S3 (Supplementary Material), C_1 conformers.

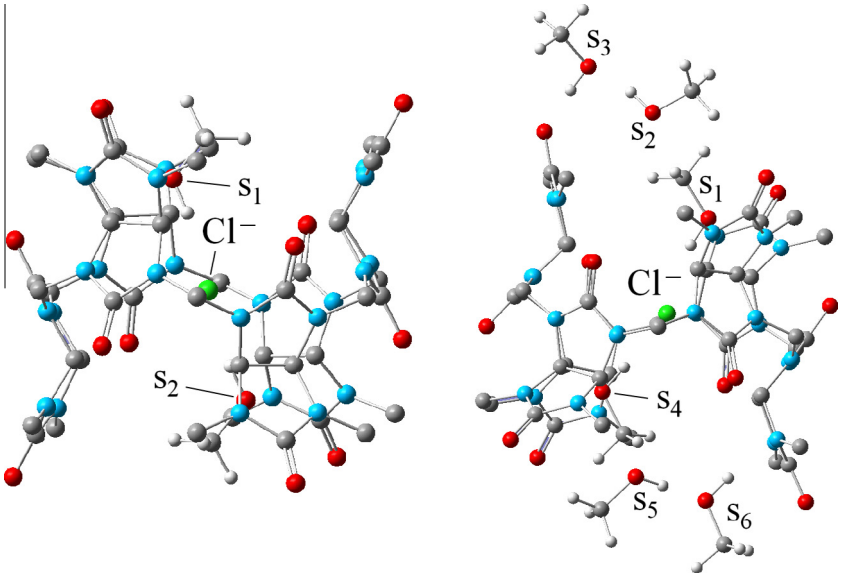

Fig. 4. Optimized geometry of Cl^-@BU[6](MeOH)$_2$ (left), and of Cl^-@BU[6](MeOH)$_6$ (right) as obtained with B3LYP/LANL2DZ. H-atoms of BU[6] have been omitted for clarity.

Table 8
Chemical shift (in ppm) of the methinic protons of X^-@BU[6](MeOH)$_n$ (X^- = Cl^-, Br^-, I^-; n = 2, 6; TMS as reference) in the presence of the solvent as obtained using B3LYP/LANL2DZ (T = 298 K).

Complex	δ_{Hc}
Cl^-@BU[6](MeOH)$_2$/CPCM	5.33
Cl^-@BU[6](MeOH)$_6$/CPCM	5.75
Br^-@BU[6](MeOH)$_2$/CPCM	5.29
Br^-@BU[6](MeOH)$_6$/CPCM	5.49
I^-@BU[6](MeOH)$_2$/CPCM	5.35
I^-@BU[6](MeOH)$_6$/CPCM	5.41

Table 9
Relative affinity of BU[6] for chloride, bromide and iodide as calculated with B3LYP/LANL2DZ in the presence of the solvent (discrete and discrete-continuum models) (T = 298 K).

Solvent model	$\Delta\Delta\delta_{X^-}$ (ppm)		
	I^-	Br^-	Cl^-
2 MeOH	0.06	−0.03	0
6 MeOH	−0.10	−0.19	0
2MeOH/C-PCM	0.02	−0.04	0
6 MeOH/C-PCM	−0.34	−0.26	0
Exp.[a]	0.19	0.05	0

[a] Taken from Ref. [5].

methinic proton, all values of δ_{Hc} being worse with respect to the ones of the discrete model.

As in the gas phase, the relative affinity of the macrocycle for halides in the presence of the solvent was investigated by means of the relative shift of the methinic proton of BU[6] with respect to host–guest complexes. As previously mentioned, the presence of the solvent herein was also taken through two approaches into account (discrete and discrete-continuum models).

Table 9 exhibits B3LYP/LANL2DZ/GIAO results, considering the ones for Cl^-@BU[6] as reference. All models were able to distinguish the effect of the halide on the resonance signal of the methinic protons. However, in practically all cases, bromide emerged as preferred guest, result in contraposition to the experimental evidence [5]. Systems with six methanol molecules point to iodide as the preferred guest in the presence of the continuum, this finding being also in disagreement with the experimental result [5]. All results displayed in Table 9 helped us in assuming that the inclusion of the solvent does not lead to any improvement of our best results in the gas phase.

3.4. Inclusion complex: F^-@BU[6] (in the gas phase and in the presence of the solvent)

This complex has been investigated in the gas phase and in the presence of methanol as solvent employing a discrete model with two and six molecules, and a hybrid discrete-continuum approach. B3LYP and M06-2X in combination with LANL2DZ, MIDI! and 6-311G have been considered for all calculations in the gas phase, and B3LYP/LANL2DZ has been used in studying the influence of the solvent models.

In the gas phase, we started from complexes with D_{3d}, S_6, and C_1 symmetries. However, all minima represent structures in which BU[6] shows important geometric deformations (Fig. 5a), leading to an inclusion complex with low symmetry. Our geometric results for F^-@BU[6] in the gas phase are in agreement with that reported by Gobre et al. using B3LYP/6-31G(d,p) [15].

The inclusion of two molecules of solvent promotes interesting geometric features (Fig. 5b and c). As in the gas phase, fluoride is located displaced from the center of the cavity in F^-@BU[6](MeOH)$_2$. This finding promotes a close interaction with four methinic proton with distances $H_{methinic}\cdots F^-$ (in Å) of 2.26, 2.34, 2.54, and 2.71, the other distances being beyond 3 Å (up to 4.3 Å).

As can be seen in Fig. 5, the presence of methanol induces structural modification of the macrocycle in minor extension with respect to F^-@BU[6]. The solvent is observed bonded with the anion *via* H-bond with a distance O–H$\cdots F^-$ of 1.56 Å. The interaction solvent$\cdots$anion appears strong enough to cause the oxygen of methanol ending co-planar with the methinic protons at both sides of the plane of fluoride. Thus, the methanol molecules could be considered as (partial) encapsulated. For comparison purposes, the optimized structures of F^-@BU[6](MeOH)$_2$ and Cl^-@BU[6](MeOH)$_2$ are depicted in Fig. 6. The addition of four solvent molecules to F^-@BU[6](MeOH)$_2$ does not introduce relevant structural changes (Fig. 5d and e).

Table 10 summarizes all ^{1}H NMR results obtained with B3LYP, and M06-2X in combination with LANL2DZ, MIDI!, and 6-311G. Our findings in the presence of the solvent (discrete and discrete-continuum models) are also included.

In the gas phase, values of δ_{Hc} in the range 5.30–5.57 ppm have been obtained with B3LYP, whilst values ranging from 5.34 to 5.45 ppm have been calculated with M06-2X. The basis set clearly appears as a variable more important in giving values of δ_{Hc} when compared with the ones observed for X^-@BU[6] (X^- = Cl^-, Br^-, I^-). It is to be noted that our results are in line with the value of 5.6 ppm calculated by Gobre et al. using B3LYP/6-31G(d,p)/DMSO [15].

The inclusion of the solvent provokes interesting results. When two water molecules are explicited, shielding of H_c is obtained with a shift of −0.09 ppm taken the B3LYP/LANL2DZ result in the gas phase into account. However, the presence of a dielectric causes a deshielding of the same signal with a shift of 0.03 ppm. This behavior is more pronounced when six solvent units are considering, both in the gas phase and in the presence of a continuum (shifts of 0.38 and 0.42 ppm, respectively).

3.5. Relative affinity of BU[6] for F^-, Cl^-, Br^-, I^-

To assess the reliability of our results in the gas phase and in the presence of the solvent, optimization and GIAO calculations on X^-@BU[6] (X^- = F^-, Cl^-, Br^-, I^-) with B3LYP/6-311++G(d,p) and M06-2X/6-311++G(d,p) were also conducted. In these cases, we included methanol as solvent (as in the experiments [5]) using the C-PCM approach [31,32].

Table 11 summarizes all results of relative affinity of the macrocycle towards halides as calculated with different DFT methodologies in the gas phase and in the presence of the solvent.

The ^{1}H NMR shift of the methinic protons of BU[6] in the presence of halides has been experimentally employed to decide the relative affinity of the macrocycle for such anions [5]. As previously discussed, we observed DFT methods unable to reproduce the affinity of the macrocycle toward chloride, bromide, and iodide. In this regard, it is to be noted that B3LYP/6-311++G(d,p) was also inadequate to simulate the reported affinity. In this case, shielding of H_c of BU[6] in the presence of bromide was obtained taken the results of Cl^-@BU[6] as reference.

All DFT methodologies in the gas phase and in the presence of the solvent do not account for the affinity of BU[6] for halide ions reported by Svec et al. [5]. In all cases, fluoride appears as the preferred guest. It is worth mentioning that this result is in line with the binding ability showed by a *p*-xylyl-based azamacrocycle for halides, as recently reported by Ahmed et al. [36].

From an energetic perspective, we were able to reproduce the observed affinity by employing M06-2X in combination with large basis set and taking the effects of the solvent into account

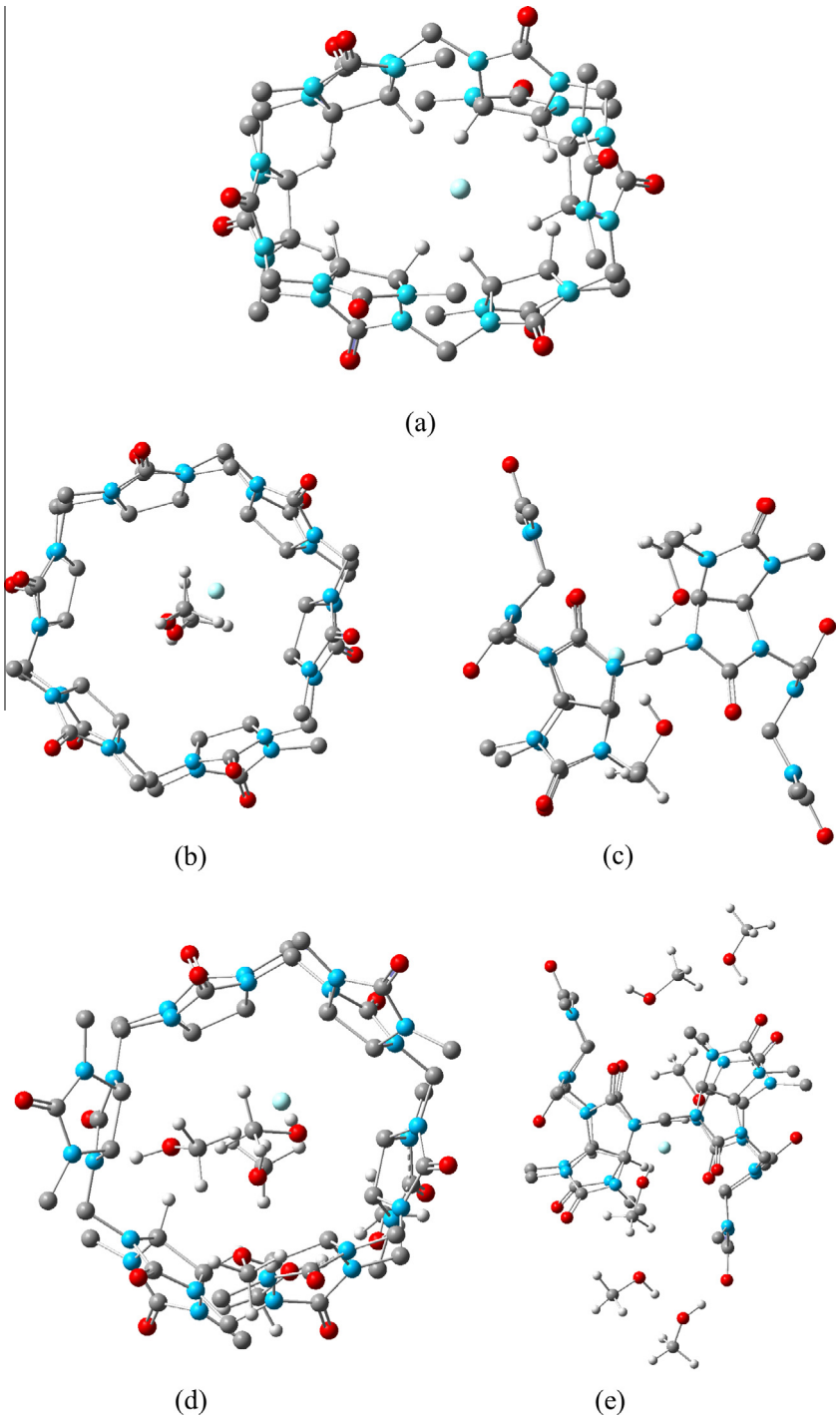

Fig. 5. B3LYP/LANL2DZ optimized geometry of: (a) F^-@BU[6]; (b) F^-@BU[6](MeOH)$_2$ (top view); (c) F^-@BU[6](MeOH)$_2$ (side view); (d) F^-@BU[6](MeOH)$_6$ (top view); (e) F^-@BU[6](MeOH)$_6$ (side view). H-atoms of BU[6] have been omitted for clarity.

[12]. However, this functional has shown a different behavior in our ^{1}H NMR investigations. Experimentally, all NMR studies have been conducted in such way that replacement of chloride for fluoride, of chloride for bromide, and of bromide for iodide has been assayed [5]. This fact implies hence, competitive experiments in which not only the relative affinity of the macrocycle for halides is involved. Variables derived from structural deformation of the host in the presence of the guest, and from the strength of solvent···anion interactions should be also considered. These variables appear as a very important in the case of fluoride, which indeed promotes all DFT methodologies used in our work to fail in simulating the relative affinity experimentally observed. When fluoride is not considered, the low-cost B3LYP/LANL2DZ resulted an excellent performer in dealing with relative affinity of host–guest complexes by means of ^{1}H NMR calculations, even in absence of the solvent.

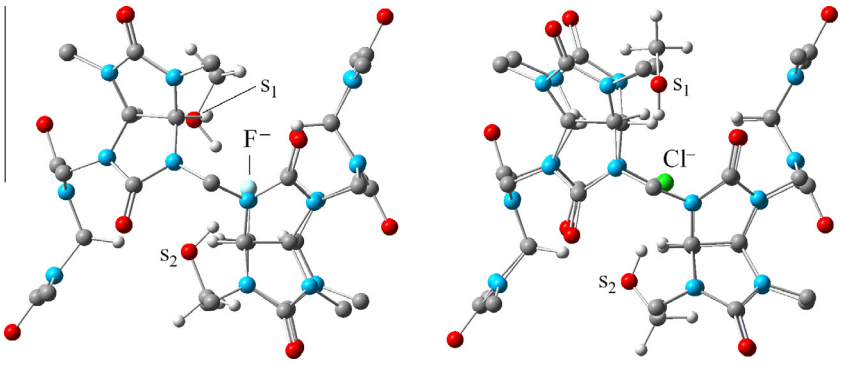

Fig. 6. B3LYP/LANL2DZ optimized geometry of F^-@BU[6](MeOH)$_2$ (left) and of Cl^-@BU[6](MeOH)$_2$ (right). Only methinic H-atoms of BU[6] have been included for clarity.

Table 10
Chemical shift (in ppm) of the methinic protons of F^-@BU[6] (TMS as reference) in the gas phase and in the presence of the solvent obtained using different functionals in combination with different basis sets (T = 298 K).

Complex	Method[a]	δ_{Hc}	$\Delta\delta_{F^-}$ [b]
F^-@BU[6]	BLDZ	5.57	0.63
	BMIDI	5.30	1.08
	B6311	5.43	0.36
	MLDZ	5.34	0.63
	MMIDI	5.45	1.02
	M6311	5.35	0.42
F^-@BU[6](MeOH)$_2$	BLDZ	5.48	0.54
F^-@BU[6](MeOH)$_6$	BLDZ	5.95	1.01
F^-@BU[6](MeOH)$_2$/CPCM	BLDZ	5.60	0.57[c]
F^-@BU[6](MeOH)$_6$/CPCM	BLDZ	5.99	0.96[c]

[a] B/M/LDZ = B3LYP/M06-2X/LANL2DZ; B/M/MIDI = B3LYP/M06-2X/MIDI!; B/M/6311 = B3LYP/M06-2X/6-311G.
[b] $\Delta\delta_{F^-} = \delta_{Hc}$ (complex) – δ_{Hc} (BU[6]).
[c] $\Delta\delta_{F^-} = \delta_{Hc}$ (complex) – δ_{Hc} (BU[6]/CPCM).

Table 11
Relative affinity of BU[6] for halide ions[a] as calculated with different DFT methodologies in the gas phase and in the presence of the solvent (discrete and discrete-continuum models) (T = 298 K).

Methodology	$\Delta\Delta\delta_{X^-}$ (ppm)[b]			
	F^-	I^-	Br^-	Cl^-
B3LYP/LANL2DZ	0.17	0.11	0.03	0
B3LYP/MIDI!	0.31	−0.22	−0.22	0
B3LYP/6-311G	0.30	0.15	0.05	0
M06-2X/LANL2DZ	0.22	0.14	0.01	0
M06-2X/MIDI!	0.30	0.03	−0.01	0
M06-2X/6-311G	0.26	0.13	0.03	0
B3LYP/6-311++G(d,p)	0.25	0.08	−0.02	0[c]
B3LYP/6-311++G(d,p)/CPCM	0.20	0.18	0.06	0[d]
M06-2X/6-311++G(d,p)	0.41	0.06	0.03	0[c]
M06-2X/6-311++G(d,p)/CPCM	0.32	0.16	0.11	0[e]
B3LYP/LANL2DZ/2 MeOH	0.11	0.06	−0.03	0
B3LYP/LANL2DZ/6 MeOH	0.20	−0.10	−0.19	0
B3LYP/LANL2DZ/2 MeOH/CPCM	0.27[f]	0.02	−0.04	0
B3LYP/LANL2DZ/6 MeOH/CPCM	0.24[g]	−0.34	−0.26	0
Exp.[h]		0.19	0.05	0

[a] The C_1 conformer has been considered for X^-@BU[6] (X^- = Cl^-, Br^-, I^-) in the gas phase.
[b] $\Delta\Delta\delta_{X^-} = (\Delta\delta_{X^-} - \Delta\delta_{Cl^-})$ (in ppm) with X^- = F^-, Cl^-, Br^-, and I^-.
[c] δ_{Hc} = 5.53 ppm.
[d] δ_{Hc} = 5.40 ppm.
[e] δ_{Hc} = 5.48 ppm.
[f] δ_{Hc} = 5.62 ppm.
[g] δ_{Hc} = 5.87 ppm.
[h] Taken from Ref. [5].

4. Conclusions

Herein, we present a DFT/GIAO investigation of the affinity of bambus[6]uril (BU[6]) towards halide ions (F^-, Cl^-, Br^-, and I^-). Our aim is to assess the reliability of low-cost DFT methodology to study relative affinity in host–guest processes in the gas phase. Complexes X^-@BU[6] (X^- = F^-, Cl^-, Br^-, I^-) were studied in the gas phase, and in the presence of the solvent by means of discrete and discrete-continuum approaches.

When BU[6] encapsulates halides (X^-), all DFT methods overestimate de magnitude of the interaction BU[6]···X^-. However, the *relative affinity* experimentally proposed was correctly described by B3LYP and M06-2X combined with LANL2DZ and 6-311G: this receptor binds such anions preferentially in the order: I^- > Br^- > Cl^-. B3LYP/LANLDZ was also in conditions to correctly account for the magnitude of the affinity, which a value almost identical to the experimental one.

B3LYP/LANL2DZ calculations on X^-@BU[6] (X^- = Cl^-, Br^-, I^-) adding two and six methanol molecules, and also considering the effects of a dielectric with ε of 32.613 (methanol as solvent) were carried out. Minor structural changes of the receptors have been observed with two solvent molecules, which have been observed at the portal of the macrocycle interacting with the anion *via* H-bond. The inclusion of six methanol units, and the inclusion of the dielectric, did not conduct to relevant geometric modification. All results with explicit solvent improve the results of δ_{Hc} in the gas phase. Indeed, an excellent result was obtained for Cl^-@BU[6](H$_2$O)$_2$, for which B3LYP/LANL2DZ gives a value of δ_{Hc} of 5.37 ppm, 0.01 ppm downfield-shifted with respect to the experimental value (5.36 ppm in CH_3OH-d_4:$CHCl_3$-d, 2:1, v:v). However, in terms of *relative affinity*, no improvement of the results in the gas phase was observed with the inclusion of the solvent (discrete and discrete-continuum models).

Host–guest complexes F^-@BU[6](MeOH)$_n$ (n = 2, 6) were studied in the gas phase and in the presence of the solvent. The absence of solvent leads to important geometric modification of the macrocycle. Even when structural modifications were also obtained by inclusion of two solvent molecules, they were no so important. The explicitation of more methanol molecules or the presence of the dielectric did not lead to remarkable changes.

The reliability of our results of relative affinity in the gas phase and in the presence of the solvent was assessed by calculations with B3LYP and M06-2X employing 6-311++G(d,p) on X^-@BU[6] (X^- = F^-, Cl^-, Br^-, I^-). While M06-2X/6-311++G(d,p) did not introduce changes to the results in the gas phase with low-cost DFT methods, B3LYP/6-311++G(d,p) has proven to be unable to correctly describe the relative affinity of BU[6] for halide ions. At the same time, all DFT methods accounted for fluoride as the preferred guest, in contraposition to the experimental finding. For this guest, variables derived from structural deformation of the host in the presence of the guest, and from the strength of solvent···anion interactions should be also considered.

When fluoride is not considered, the low-cost B3LYP/LANL2DZ resulted an excellent performer in dealing with relative affinity

of host–guest complexes by means of ^{1}H NMR calculations, even in absence of the solvent.

Finally, we recommended B3LYP/LANL2DZ/GIAO in the gas phase as a reliable tool to assist experimentalists in studying relative affinities in encapsulation processes of similar guests keeping the computational cost very low.

Acknowledgments

We thank PEDECIBA-QUIMICA and ANII (Agencia Nacional de Invstigación e Innovación) for financial support.

Appendix A. Supplementary material

Supplementary data associated with this article can be found, in the online version, at http://dx.doi.org/10.1016/j.comptc.2015.03.028.

References

[1] M. Grzelczak, J. Vermant, E.M. Furst, L.M. Liz-Marzán, Directed self-assembly of nanoparticles, ACS Nano 4 (2010) 3591–3605.
[2] X. Yan, S. Li, T.R. Cook, X. Ji, Y. Yao, J.B. Pollock, Y. Shi, G. Yu, J. Li, F. Huang, P.J. Stang, Hierarchical self-assembly: well-defined supramolecular nanostructures and metallohydrogels via amphiphilic discrete organoplatinum(II) metallacycles, J. Am. Chem. Soc. 135 (2013) 14036–14039.
[3] J. Lagona, J. Mukhopadhyay, S. Chakrabarti, L. Isaacs, The cucurbit[n]uril family, Angew. Chem. Int. Ed. 44 (2005) 4844–4870.
[4] M. Raynal, P. Ballester, A. Vidal-Ferran, P.W.N.M. van Leeuwen, Supramolecular catalysis. Part 1: non-covalent interactions as a tool for building and modifying homogeneous catalysts, Chem. Soc. Rev. 43 (2014) 1660–1733. and references therein.
[5] J. Svec, M. Necas, V. Sindelar, Bambus[6]uril, Angew. Chem. Int. Ed. 49 (2010) 2378–2381.
[6] W.H. Huan, P.Y. Zavalij, L. Isaacs, Chiral recognition inside a chiral cucurbituril, Angew. Chem. Int. Ed. 46 (2007) 7425–7427.
[7] K. Kim, N. Selvapalam, Y.H. Ko, K.M. Park, D. Kim, J. Kim, Functionalized cucurbiturils and their applications, Chem. Soc. Rev. 36 (2007) 267–279.
[8] R. Behrend, E. Meyer, F.I. Rusche, Ueber condensationsproducte aus glycoluril und formaldehyd, Ann. Chem. 339 (1905) 1–37.
[9] W.A. Freeman, W.L. Mock, N.Y. Shih, Cucurbituril, J. Am. Chem. Soc. 103 (1981) 7367–7368.
[10] J.W. Lee, S. Samal, N. Selvapalam, H.J. Kim, K. Kim, Cucurbituril homologues and derivatives: new opportunities in supramolecular chemistry, Acc. Chem. Res. 36 (36) (2003) 621–630. and references therein.
[11] J. Svec, M. Dusek, K. Fejfarova, P. Stacko, P. Klan, A.E. Kaifer, W. Li, E. Hudeckova, V. Sindelar, Anion-free bambus[6]uril and its supramolecular properties, Chem. Eur. J. 17 (2011) 5605–5612.
[12] P.A. Denis, J.S. Gancheff, On the encapsulation of halide anions by bambus[6]uril, Comp. Theor. Chem. 1023 (2013) 5–9.
[13] P.A. Denis, J.S. Gancheff, Coupled cluster and density functional investigation of the hydrogen bond between halides, paraffines, olefins, and alkynes, Struct. Chem. 25 (2014) 903–908.
[14] P. Toman, E. Makrlík, P. Vaňura, Theoretical study on the complexation of bambus[6]uril with the fluoride anion, Comp. Theor. Chem. 989 (2012) 97–99.
[15] V.V. Gobre, P.H. Dixit, J.K. Khedkar, S.P. Gejji, Electronic structure, vibrational spectra and ^{1}H NMR of halide ion (F^-, Cl^- and Br^-) encapsulated bambus[6]uril from density functional theory, Comp. Theor. Chem. 976 (2011) 76–82.
[16] P. Toman, E. Makrlík, P. Vaňura, Theoretical study on the complexation of bambus[6]uril with the chloride, bromide, and iodide anions, Monatsh. Chem. 142 (2011) 881–884.
[17] R. Jain, T. Bally, P.R. Rablen, Calculating accurate proton chemical shifts of organic molecules with density functional methods and modest basis sets, J. Org. Chem. 74 (2009) 4017–4023.
[18] A.D. Becke, Density-functional exchange-energy approximation with correct asymptotic behavior, Phys. Rev. A 38 (1988) 3098–3100.
[19] A.D. Becke, A new mixing of Hartree–Fock and local density-functional theories, J. Chem. Phys. 98 (1993) 1372–1377.
[20] Y. Lee, W. Yang, R.G. Parr, Development of the Colle-Salvetti correlation-energy formula into a functional of the electron density, Phys. Rev. B 37 (1988) 785–789.
[21] Y. Zhao, D.G. Truhlar, A new local density functional for main-group thermochemistry, transition metal bonding, thermochemical kinetics, and noncovalent interactions, J. Chem. Phys. 125 (2006) 194101–194118.
[22] Y. Zhao, D.G. Truhlar, The M06 suite of density functionals for main group thermochemistry, thermochemical kinetics, noncovalent interactions, excited states, and transition elements: two new functionals and systematic testing of four M06-class functionals and 12 other functionals, Theor. Chem. Acc. 120 (2008) 215–241.
[23] Y. Zhao, N.E. Schultz, D.G. Truhlar, Design of density functionals by combining the method of constraint satisfaction with parametrization for thermochemistry, thermochemical kinetics, and noncovalent interactions, J. Chem. Theory Comput. 2 (2006) 364–382.
[24] Y. Zhao, D.G. Truhlar, Size-selective supramolecular chemistry in a hydrocarbon nanoring, J. Am. Chem. Soc. 129 (2007) 8440–8442.
[25] J.R. Cheeseman, G.W. Trucks, T.A. Keith, M.J. Frisch, A comparison of models for calculating nuclear magnetic resonance shielding tensors, J. Chem. Phys. 104 (1996) 5497–5509.
[26] M.W. Lodewyk, M.R. Siebert, D.J. Tantillo, Computational prediction of ^{1}H and ^{13}C chemical shifts: a useful tool for natural product, mechanistic, and synthetic organic chemistry, Chem. Rev. 112 (2012) 1839–1862.
[27] F. London, Théorie quantique des courants interatomiques dans les combinaisons aromatiques, J. Phys. Rad. 8 (1937) 397–409.
[28] R. McWeeny, Perturbation theory for the Fock-Dirac density matrix, Phys. Rev. 126 (1962) 1028–1034.
[29] R. Ditchfield, Self-consistent perturbation theory of diamagnetism. I. A gauge-invariant LCAO method for N.M.R. chemical shifts, Mol. Phys. 27 (1974) 789–807.
[30] K. Wolinski, J.F. Hilton, P. Pulay, Efficient implementation of the gauge-independent atomic orbital method for NMR chemical shift calculations, J. Am. Chem. Soc. 112 (1990) 8251–8260.
[31] V. Barone, M. Cossi, Quantum calculation of molecular energies and energy gradients in solution by a conductor solvent model, J. Phys. Chem. A 102 (1998) 1995–2001.
[32] M. Cossi, N. Rega, G. Scalmani, V. Barone, Energies, structures, and electronic properties of molecules in solution with the C-PCM solvation model, J. Comput. Chem. 24 (2003) 669–681.
[33] M.J. Frisch, G.W. Trucks, H.B. Schlegel, G.E. Scuseria, M.A. Robb, J.R. Cheeseman, G. Scalmani, V. Barone, B. Mennucci, G.A. Petersson, H. Nakatsuji, M. Caricato, X. Li, H.P. Hratchian, A.F. Izmaylov, J. Bloino, G. Zheng, J.L. Sonnenberg, M. Hada, M. Ehara, K. Toyota, R. Fukuda, J. Hasegawa, M. Ishida, T. Nakajima, Y. Honda, O. Kitao, H. Nakai, T. Vreven, J.A. Montgomery, Jr., J.E. Peralta, F. Ogliaro, M. Bearpark, J.J. Heyd, E. Brothers, K.N. Kudin, V.N. Staroverov, R. Kobayashi, J. Normand, K. Raghavachari, A. Rendell, J.C. Burant, S.S. Iyengar, J. Tomasi, M. Cossi, N. Rega, J.M. Millam, M. Klene, J.E. Knox, J.B. Cross, V. Bakken, C. Adamo, J. Jaramillo, R. Gomperts, R.E. Stratmann, O. Yazyev, A.J. Austin, R. Cammi, C. Pomelli, J.W. Ochterski, R.L. Martin, K. Morokuma, V.G. Zakrzewski, G.A. Voth, P. Salvador, J.J. Dannenberg, S. Dapprich, A.D. Daniels, O. Farkas, J.B. Foresman, J.V. Ortiz, J. Cioslowski, D.J. Fox, Gaussian Inc., Wallingford, CT, 2009.
[34] J.C. Espinoza-Hicks, A.A. Camacho-Dávila, N.R. Flores-Holguín, G.V. Nevárez-Moorillón, D. Glossman-Mitnik, L.M. Rodríguez-Valdez, Experimental and quantum chemical studies of a novel synthetic prenylated chalcone, Chem. Cent. J. 7 (2013) 17–28.
[35] P.H. Dixit, R.V. Pinjari, S.P. Gejji, Electronic structure and ^{1}H NMR chemical shifts in host-guest complexes of cucurbit[6]uril and sym-tetramethyl cucurbit[6]uril with imidazole derivatives, J. Phys. Chem. A 114 (2010) 10906–10916.
[36] L. Ahmed, M.M. Rhaman, J.S. Mendy, J. Wang, F.R. Fronczek, D.R. Powell, J. Leszczynski, M.A. Hossain, Experimental and theoretical studies on halide binding with a *p*-Xylyl-based azamacrocycle, J. Chem. Phys. A 119 (2015) 383–394.